ELSEVIER Science Press

Trans. Nonferrous Met. Soc. China 19(2009) s157−s163

Transactions of Nonferrous Metals Society of China

www.tnmsc.cn

Influence of process parameters on drilling characteristics of Al 1050 sheet with thickness of 0.2 mm using pulsed Nd:YAG laser

Dong-Gyu AHN, Gwang-Won JUNG

Department of Mechanical Engineering, Chosun University, 375 Seosuk-dong, Dong-gu, Gwang-ju, 501-759, Korea

Received 2 March 2009; accepted 30 May 2009

Abstract: The object of this work is to investigate the influence of process parameters on drilling characteristics of an Al 1050 sheet with a thickness of 0.2 mm using a pulsed Nd:YAG laser through numerical analyses and experiments. By comparing the numerical analyses with the experiments, a proper numerical model was obtained. From the results of the numerical analyses and the experiments, the effects of process parameters on entrance diameters of drilled holes, shapes of the holes, taper angles of the holes and temperature distributions in the vicinity of the holes were examined quantitatively. In addition, the optimal drilling condition was estimated to improve the quality of the drilled holes.

Key words: Al 1050 sheet; pulsed Nd:YAG laser; process parameters; drilled hole formation; temperature distribution; optimal drilling condition

1 Introduction

Laser material processing technology has been used to manufacture desired parts rapidly using subtractive and addictive methodology[1−2]. Recently, the application field of the laser drilling process has been extended due to the growth in the market of electronics, computers, communication products, and automotive parts[3−4]. The non-contact machining characteristics of the laser drilling process can reduce appreciably problems related to mechanical piercing and boring of thin sheets, such as serious deformation of the cut part, eccentricity of the hole and crumbling of the cut section, induced by direct contact of tools with the sheet metal [3, 5]. The merits of a Nd:YAG laser, including a high energy density, distinguished focusing characteristics, a narrower heat affected zone, a better hole edge profile, and the capability of the enhanced transmission through plasma, make it an interesting application for precise sheet metal drilling[1].

Thin aluminum sheets have been used in the manufacture of printed circuit boards with many meso- or micro-holes and in the fabrication of mobile phones that require a number of small holes. The aluminum sheet has inherent limitations, including the high reflectivity, high conductivity and the distinguished oxidation reaction, in terms of laser material processing [4, 6]. The well-known manufacturing technologies of meso- and micro-parts incorporating aluminum include electrochemical machining, photolithography and micro-electro-discharge machining[6−7]. Recent advances in laser systems have enabled the laser to drill meso- and micro-holes in aluminum sheets[6].

In a laser drilling process, the productivity of the product and the quality of the drilled hole are dependent on the combination of the process parameters, including the laser power, the pulse duration time, the pulse frequency, the focal distance, and the nozzle diameter[1]. TUNNA et al[6] researched the effects of the intensity, wave length and spot diameter of the laser on the average etch depth per pulse and the hole geometry in the drilling of pure aluminum sheets using a pulsed Nd:YAG laser. GHOREISHI et al[8] investigated the relationships and parameter interactions between six controllable variables, including laser peak power, laser pulse width, pulse frequency, number of laser pulses, assist gas pressure, and focal plane position, on the hole taper and circularity in the laser percussion drilling of a stainless steel using a pulsed YAG laser. During the laser drilling of the material, a thermal field of the material is formed continuously in the thickness direction[9−10]. The thermal field is highly influenced by the arrangement of the process parameters. The temperature distribution in

Corresponding author: Dong-Gyu AHN; Tel: +82-62-230-7043; Fax: +82-62-230-7234; E-mail: smart@mail.chosun.ac.kr

the thermal field provides useful information for controlling the dimension and shape of the drilled hole[11]. SOLANA et al[12] provided a model to analyze the drilling speeds and hole profiles for various types of laser sources. They also estimated the required energy to drill a hole according to the thickness of a titanium plate and the variation of hole profiles according to the focal position and the applied energy. PETKOVSEK et al[13] studied the influence of consecutive pulse numbers on the hole depth in the laser drilling of different materials using a numerical analysis.

The objective of the present study is to investigate the influence of process parameters, including the duration time and the frequency of the pulse, on drilling characteristics and to obtain the optimal drilling condition in the drilling of an Al 1050 sheet with a thickness of 0.2 mm using a pulsed Nd:YAG laser. Transient heat transfer analyses considering the variation of material properties according to the temperature were performed using a commercial code ABAQUS to examine the effects of the duration time and the frequency of the pulse on temperature distributions in the vicinity of the applied region of a laser beam. Laser drilling experiments were performed using a PC-NC controlled laser drilling system with pulsed Nd:YAG laser to investigate the variation of the diameter, the shape and the taper angle of the drilled hole according to the drilling condition. The diameter, shape and the taper angle of the drilled hole were measured via a scanning electron microscope(SEM). By comparing the results of numerical analyses and those of experiments, the validity of the numerical analyses were discussed. Finally, the optimal drilling condition was estimated to improve the quality of the drilled hole.

2 Numerical analyses

In order to investigate the influence of the process parameters on the temperature distribution in an Al 1050 sheet with a thickness of 0.2 mm during a drilling using a pulsed Nd:YAG laser, a three-dimensionally transient heat transfer analysis was carried out using the commercial software ABAQUS V6.5. In the numerical analysis, the process parameters were chosen as the duration time and the frequency of the pulse of the laser. The region of analysis was selected as ±3.0 mm from the center of the heat source in the radial direction, as shown in Fig.1. The analysis region was represented by 1 947 nodes and 1 680 hexahedral elements. A biased mesh structure, in which the meshes are concentrated on the center of the heat source as well as on the upper and bottom surface of the workpiece, was introduced to consider rapid changes of temperature distributions in the vicinity of the irradiated region of the laser and external surfaces of workpiece during the laser material processing, as shown in Fig.1.

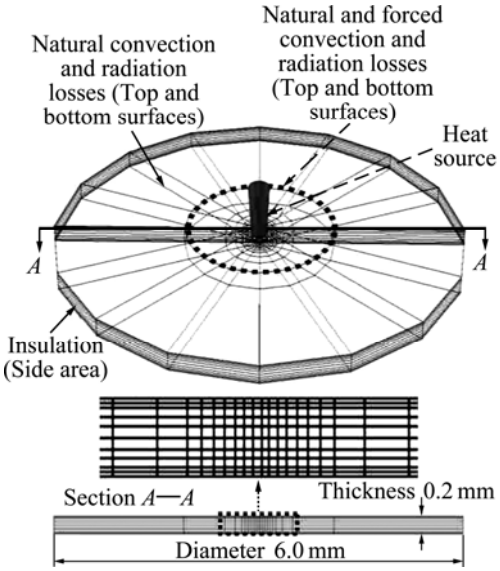

Fig.1 Mesh structure and boundary condition of transient heat transfer analysis

The thermal conductivity, specific heat and density of the workpiece were considered to be temperature-dependent, as shown in Fig.2(a). The melting point and vaporization temperature of Al 1050 are 933 K and 2 740 K, respectively. Natural convection and radiation conditions were applied to the entire external surface of the analysis model. In addition, a forced convection condition was applied to the projected region of the assisted gas. The coefficients of the natural and forced convections were set to be 10 W/(m^2·K) and 4 464 W/(m^2·K), respectively. The emissivity of Al 1050 was set to be 0.09. The region, in which the temperature of the workpiece is greater than the melting point of the Al 1050, was assumed to be the drilled region in the numerical analysis.

The laser was assumed as a surface heat flux model with a Gaussian distribution of intensity, as shown in Eq.(1). As it is difficult to create a physical model with accurate intensity of the evaporation heat in a numerical analysis, the efficiency of the heat flux(η) was introduced. The efficiency of the heat flux was estimated through a comparison of the results of the experiments and those of the numerical analyses. The absorption coefficient(α) of the workpiece was set to be 0.2 according to the report of PIERRON et al[4]. The spot radius(R) of the pulsed Nd:YAG laser was 0.2 mm.

$$I(r)=\eta\alpha\frac{2}{\pi R^2}\frac{P_{\mathrm{m}}}{t_{\mathrm{p}}F}\exp\left\{-2\left(\frac{r}{R}\right)^2\right\} \quad (1)$$

where $I(r)$, r, η, α, P_{m}, t_{p}, F and R are the intensity

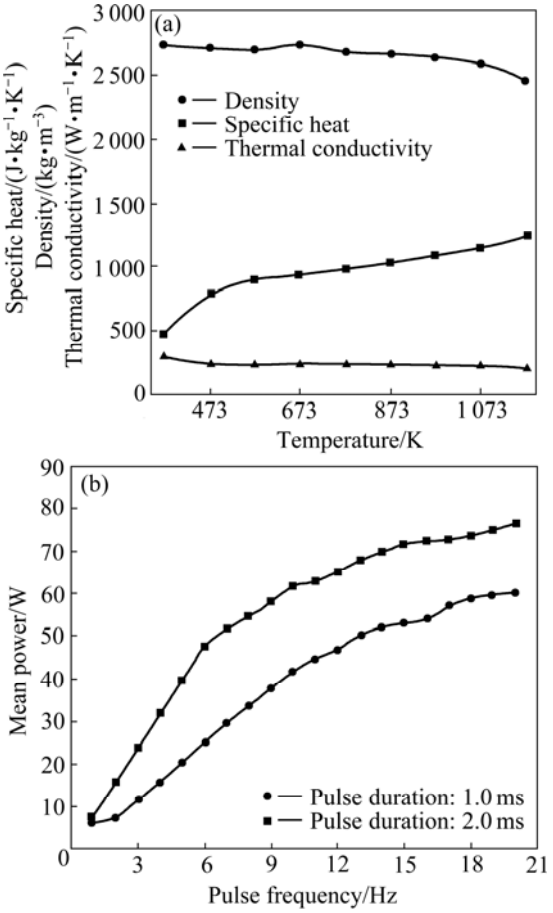

Fig.2 Mean power of laser and thermal properties of Al 1050: (a) Variation of density, specific heat and thermal conductivity of Al 1050 according to temperature; (b) Variation of mean power of laser according to duration time and frequency of pulse (Input voltage 400 V)

distribution of laser per unit pulse, the radial distance from the center of the laser beam, the efficiency, the absorption coefficient of Al 1050, the mean power of the laser, the duration time of the pulse, the frequency of the pulse and the spot radius of the laser, respectively.

The mean power of the laser was measured by a power meter (COHERENT Inc., PM150), as shown in Fig.2(b). The input voltage of the laser was 400 V. The duration time and the frequency of the laser were chosen as 1.0−2.0 ms and 4−12 Hz, respectively. The diameter of the nozzle was set to be 0.7 mm. The helium gas was employed as the assisted gas to remove the oxidation reaction. Hence, the oxidation reaction was not considered in the numerical analyses. The dynamic pressure at the nozzle tip was measured to estimate the velocity of the assist gas. The estimated velocity of the assisted gas was 345 m/s. Table 1 shows the condition of the numerical analyses. The diameter was measured at the entrance of the hole. The taper angle was estimated by Eq.(2).

Table 1 Conditions of numerical analyses

Input voltage/V	Duration time/ms	Frequency/ Hz	Nozzle diameter/ mm	Velocity of assisted gas/ ($m \cdot s^{-1}$)
400	1.0	4−12	0.7	345
	2.0	4−12	0.7	345

$$\varphi = 90 - \frac{180}{\pi}\tan^{-1}\left(\frac{2t}{d_{en} - d_e}\right) \quad (2)$$

where φ, t, d_{en} and d_e are the taper angle, the thickness of workpiece, the entrance diameter of the hole, and the exit diameter of the hole, respectively.

3 Experimental

Fig.3 illustrates the experimental set-up of the laser drilling experiments. Laser drilling experiments were carried out using a PC-NC based automatic laser drilling system. A pulsed Nd:YAG laser with a maximum peak power of 150 W was utilized. The transverse mode, the wavelength and the spot size of the laser were TEM_{00} mode, 1.064 μm and 0.4 mm, respectively. The focal distance was set to be 6.0 mm. The focal distance with the minimum diameter and a feasible concentricity of the hole was determined through preliminary tests. Specimens with a length of 150 mm and a width of 150 mm were manufactured from an Al 1050 sheet. The thickness of the specimen was 0.2 mm. The chemical composition of the Al 1050 sheet is 99.90% of Al, 0.038% of Fe, 0.03% of Si, and 0.002% of Cu. The experimental conditions were identical to those of the numerical analyses, as shown in Table 1. The shape, diameter and taper angle of the drilled hole were observed by SEM and optical microscope. The taper angle of the hole was estimated through the direct angle measurement of the polished cross-section of the drilled

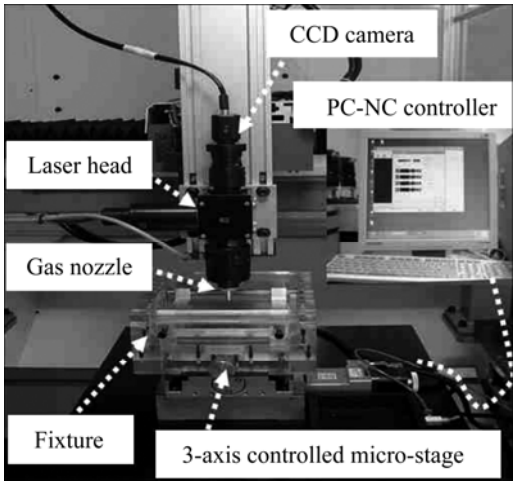

Fig.3 Experimental set-up of laser drilling experiments

hole. The optimal drilling condition was obtained through the comparison of the analytical and experimental results.

4 Results and discussion

4.1 Entrance diameter of hole and temperature distribution in vicinity of hole

Fig.4 shows the influences of the process parameters on the temperature distribution and the diameter on the top surface of the workpiece.

The analytical and experimental results showed a good agreement in terms of the entrance diameter of the drilled hole, as shown in Figs.4(a), (b), (c) and (e). These figures show that the melted region and the entrance diameter of the drilled hole increase as the duration time of the pulse increases. This may be ascribed to the fact that the increased mean power of the laser, which is induced by additional duration time, as well as additional interaction time between the workpiece and the laser, increase the heat input applied to workpiece. The increased heat input subsequently creates a wide melted region in the radial direction in comparison with the thickness direction.

The entrance diameter of the drilled hole increased appreciably in proportion to the increase of the pulse frequency, as shown in Fig.4(e). This occurred because the increase of the pulse frequency accumulated the heat input applied to the workpiece.

Fig.4(d) shows that the workpiece is not drilled

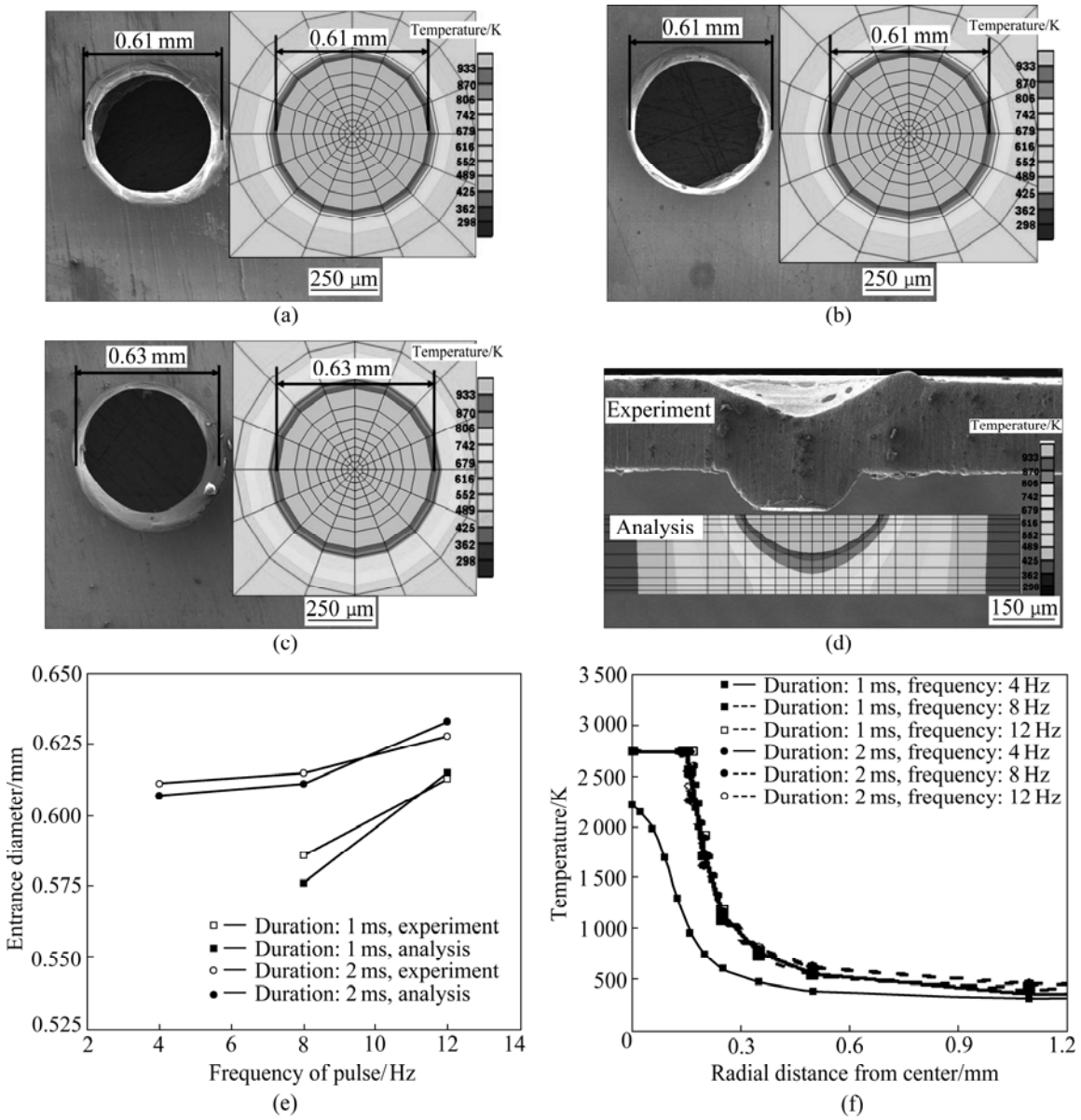

Fig.4 Influence of process parameters on temperature distribution and hole diameter: (a) Duration time 1 ms, frequency 12 Hz; (b) Duration time 2 ms, frequency 4 Hz; (c) Duration time 2 ms, frequency 12 Hz; (d) Duration time 1 ms, frequency 4 Hz; (e) Variation of entrance diameter; (f) Temperature distribution in radial direction at maximum temperature

when the duration time and frequency of the pulse are 1 ms and 4 Hz, respectively. Through the observation of the temperature distribution in the workpiece, as depicted in Fig.4(f), it was observed that the maximum temperature of the top surface is less than the vaporization temperature of Al 1050 when the duration time and frequency of the pulse are 1 ms and 4 Hz, respectively. These results imply that the undrilling of the workpiece results from the insufficient heat input to initiate the ablation of the top surface of the workpiece.

Fig.4(e) shows that the entrance diameter of the drilled hole ranges from 0.58 mm to 0.63 mm. The results of the numerical analysis show that the temperature in the workpiece decreases rapidly within 0.5 mm from the center of the heat flux in the radial direction. Through an observation of the variation of the temperature distribution according to the operation time of the laser, it was found that the cooling rate of the workpiece increases when the duration time of the pulse decreases.

4.2 Hole shape and taper angle

Figs.5 and 6 show the effects of the process parameters on the cross-section shape and the taper angle of the drilled hole.

The results of the numerical analysis were compared with those of the experiment from the viewpoint of the edge profile of the drilled hole, as shown in Fig.5(a). The comparison results showed that the edge profile of the numerical analysis is similar to that of the experiment exclusive of the dross attached region on the bottom surface, as shown in Fig.5(a). The numerical analysis could not, however, properly estimate the edge

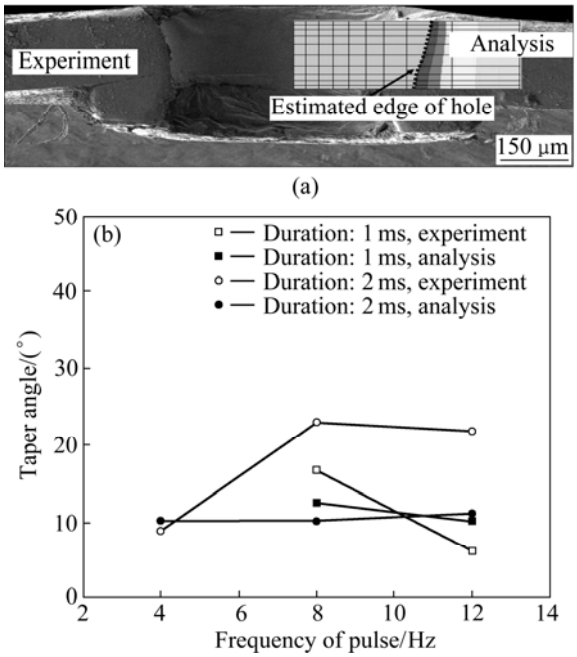

Fig.5 Comparison of results of numerical analyses and those of experiments: (a) Cross-section shape (Duration time 2 ms, frequency 4 Hz); (b) Taper angles

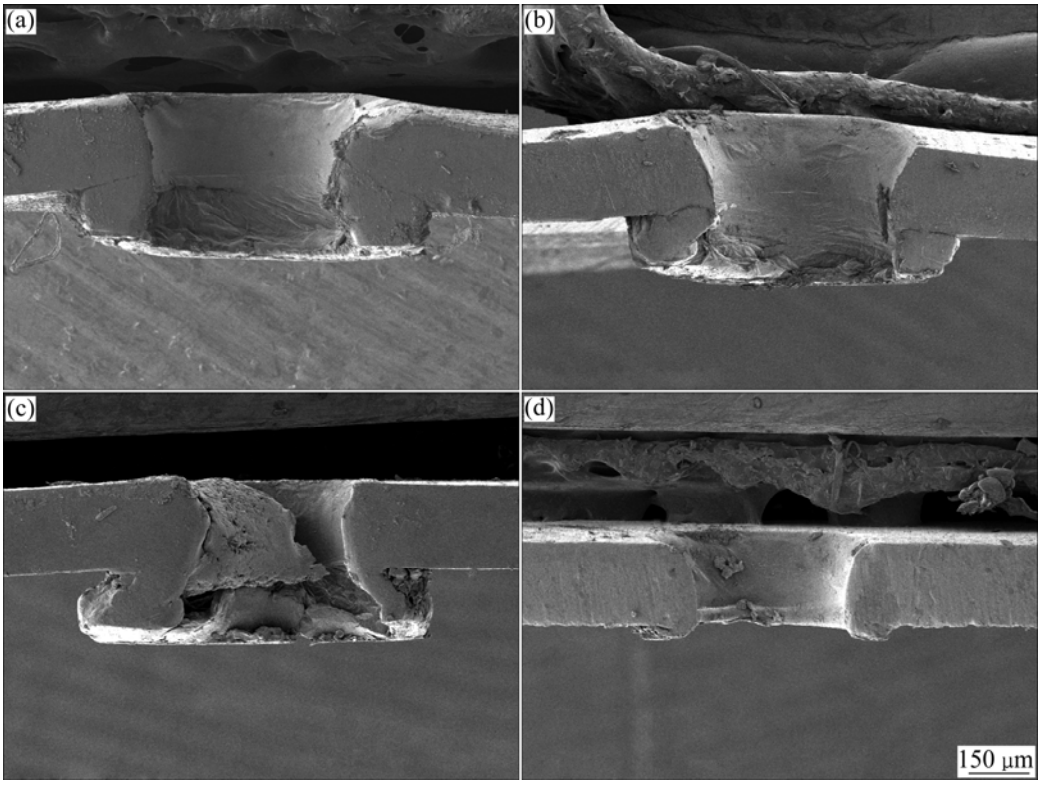

Fig.6 Variation of cross-section of drilled hole: (a) Duration time 2 ms, frequency 4 Hz; (b) Duration time 2 ms, frequency 12 Hz; (c) Duration time 1 ms, frequency 8 Hz; (d) Duration time 1 ms, frequency 12 Hz

profile of a hole in the dross attached region because the dynamic mass transfer phenomenon induced by the flow of the molten material was not considered. Hence, the taper angle of the drilled hole was measured within the thickness of the workpiece.

The experimental results also showed that a drilled hole with a guourd-shaped cross-section was created and the taper angle of the drilled hole ranged from 6° to 23°, as shown in Fig.5(b).

By comparing Fig.5 with Fig.6, it is observed that the taper angle of the drilled hole is minimized as the dross attachment and the edge breakage disappear from the bottom surface of the workpiece. Fig.5(b) and Fig.6(d) show that the desired cross-section of the drilled hole with the minimum taper angle and dross attachment is created when the duration time and the frequency of the pulse are 1 ms and 12 Hz, respectively. However, the breakage at the bottom edge of the hole is augmented appreciably, as shown in Fig.6(c), when the duration time and the frequency of the pulse are 1 ms and 8 Hz, respectively.

The experimental results show that the dross attachment increases as the duration time of the pulse increases, as depicted in Figs.6(a) and (b). This results from the fact that an increased amount of mushy phase material with a high viscosity, as induced by the increased laser power and the laser interaction time with the workpiece, in the vicinity of the drilled hole becomes attached to the bottom surface of the workpiece due to the continuous cooling of the mushy phase material during the drop down of the material along the hole surface. In addition, these figures show that the dross attachment is augmented as the pulse frequency increases.

Ejection of the melted materials on the top surface scarcely occurred under the experimental conditions, as shown in Fig.6. Melt erosion of the side walls of the drilled hole was, however, initiated when the pulse frequency was lower than 8 Hz and the pulse duration time was 1 ms, as shown in Fig.6(c).

From the above results, the optimal drilling condition was determined at a pluse duration time of 1 ms and a pulse frequency of 12 Hz. In addition, it was confirmed that a drilled hole with a taper angle of 6° and an entrance diameter of 0.61 mm can be created at the optimal drilling condition.

5 Conclusions

1) The analytical and experimental results of the drilling of an Al 1050 sheet using a pulsed Nd:YAG laser showed that the variation of the entrance diameter of the drilled hole is highly influenced by the duration time and the frequency of the pulse. In addition, it was found that the entrance diameter of the drilled hole ranges from 0.58 to 0.63 mm under both analytical and experimental conditions.

2) The results of the numerical analyses showed that an Al 1050 sheet with a thickness of 0.2 mm is not drilled when the duration time and frequency of the pulse are 1 ms and 4 Hz, respectively. Moreover, it was noted that the temperature in the workpiece changes rapidly within 0.5 mm from the center of the heat flux in the radial direction.

3) Comparison results of the analysis and the experiment showed that the edge profile of the numerical analysis is nearly similar to that of the experiment exclusive of the dross attached region on the bottom surface. In addition, it was observed that a drilled hole with a gourd-shaped cross-section is created and the taper angle of the drilled hole ranges from 6° to 23°.

4) The experimental results showed that the desired cross-section of a drilled hole with a minimum taper angle is created when the duration time and frequency of the pulse are 1 ms and 12 Hz, respectively. In addition, it was found that the dross attachment, the edge breakage and the incidence of melt erosion disappear from the vicinity of the drilled hole in the drilling condition.

5) Based on these results, the optimal cutting condition, at which the taper angle and the defects of the drilled hole are minimized, was estimated in effort to improve the quality of the drilled hole. In addition, it was confirmed that a drilled hole with a taper angle of 6° and an entrance diameter of 0.61 mm can be created under the optimal drilling condition.

Acknowledgement

This research work was supported by a grant-in-aid of Regional Innovation Center (RIC), New Technology Development and Research Center of Laser Application in Chosun University, Korea.

References

[1] DUBEY A K, YADAVA V. Experimental study of Nd:YAG laser beam machining—An overview [J]. Journal of Materials Processing Technology, 2008, 195: 15−26.

[2] LONG Ri-sheng, LIU Wei-jun, XING Fei, WANG Hua-bing. Numerical simulation of thermal behavior during laser metal deposition shaping [J]. Trans Nonferrous Met Soc China, 2008, 18(3): 691−699.

[3] WANG A H, WANG W Y, BAI Z K, XIE C S, ZENG D W, SONG W L. YAG laser percussion drilling of a functional multi-layer thin plate [J]. Optics & Laser Technology, 2007, 39: 840−845.

[4] PIERRON N, SALLAMAND P, MATTEI S. Study of magnesium and aluminum alloys absorption coefficient during Nd:YAG laser

interaction [J]. Applied Surface Science, 2007, 253: 3208−3214.

[5] KHAN A H, CELOTTO S, TUNNA L, O'NEILL W, XUTCLIFFE C J. Influence of microsupersonic gas jets on nanosecond laser percussion drilling [J]. Optics and Lasers in Engineering, 2007, 45: 709−718.

[6] TUNNA L, O'NEILL W, KHAN A, SUTCLIFFE C. Analysis of laser micro drilled holes through aluminum for micro-manufacturing applications [J]. Optics and Lasers in Engineering, 2005, 43: 937−950.

[7] THORNELL G, JOHANSSON S. Micro processing at the fingertips [J]. Journal of Micromechanics and Microengineering, 1998, 8: 251−262.

[8] GHOREISHI M, LOW D. K. Y, LI L. Comparative statistical analysis of hole taper and circularity in laser percussion drilling [J]. International Journal of Machine Tools & Manufacture, 2002, 42: 985−995.

[9] GANESH R K, FAGHRI A, HAHN Y. A generalized thermal modeling for laser drilling process (II): Numerical simulation and results [J]. International Journal of Heat and Mass Transfer, 1997, 40: 3361−3373.

[10] YILBS B S, MANSOOR S B. Laser pulse heating and phase changes in the irradiated region: Temperature-dependent thermal properties case [J]. International Journal of Thermal Sciences, 2009, 48: 761−772.

[11] NG G K L, CROUSE P L, LI L. An analytical model for laser drilling incorporating effects of exothermic reaction, pulse width and hole geometry [J]. International Journal of Heat and Mass Transfer, 2006, 49: 1358−1374.

[12] SOLANA P, KAPADIA P, DOWDEN J W, MARSDEN P J. An analytical model for the laser drilling of metals with absorption within the vapour [J]. Journal of Physcis D: Applied Physics, 1999, 32: 942−952.

[13] PETKOVSEK R, PANJAN I, BABNIK A, MOZINA J. Optodynamic study of multiple pulse micro drilling [J]. Ultrasonics, 2006, 44: e1191−e1194.

(Edited by YANG Hua)